MOLECULAR AND CELLULAR BIOLOGY, Dec. 1990, p. 6700–6708
0270-7306/90/126700-09$02.00/0

Vol. 10, No. 12

Regulation of N-*myc* Gene Expression: Use of an Adenovirus Vector To Demonstrate Posttranscriptional Control

LEE E. BABISS[1] AND JEFFREY M. FRIEDMAN[2]*

Laboratory of Molecular Cell Biology[1] and Howard Hughes Medical Institute,[2] The Rockefeller University, Box 279, 1230 York Avenue, New York, New York 10021-6399

Received 3 May 1990/Accepted 4 September 1990

We present evidence that differences in the levels of N-*myc* mRNA among different cell types are the result of posttranscriptional control. First, we noted that while steady-state mouse N-*myc* mRNA could be detected only in fetal mouse brain, it was transcribed at an equivalent rate in adult brain, liver, spleen, and placenta and in fetal brain. Similarly, the human N-*myc* gene was transcribed at an equivalent rate in HeLa cells, which do not accumulate this RNA in the cytoplasm, and cell lines G401 (a Wilms tumor-derived cell line) and SKNMc (established from a primitive neuroepithelioma), which do express N-*myc* RNA. As expected, the N-*myc* promoter functioned at equivalent rates, as demonstrated by the level of a reporter gene, when introduced into these cell types by using a recombinant adenovirus vector. The suggestion that posttranscriptional mechanisms control the level of this RNA was supported by the observation that sequences in the N-*myc* third exon specifically decreased the level of E1A mRNA when these sequences were placed downstream of the E1A promoter in a recombinant adenovirus. Finally, we further localized these sequences to a 600-bp fragment of the third exon by introducing various subclones of this sequence downstream of the E1A promoter in both viral and plasmid vectors.

N-*myc* is a cellular gene that was originally isolated as an amplified sequence in neuroblastoma cells and was found to be structurally related to the c-*myc* proto-oncogene (17, 18, 24, 25). While c-*myc* gene expression has been demonstrated in a large number of cell types, expression of N-*myc* mRNA is restricted in its tissue distribution (9, 13, 31, 32). This property of N-*myc* is a feature of other genes in the *myc* gene family, since additional members, including L-*myc* and R-*myc*, display restricted tissue cell distributions (21).

The N-*myc* gene is expressed during mouse development at high levels in neonatal brain, kidney, and intestine (9, 31, 32). Relatively high levels of N-*myc* mRNA can also be detected in some other neonatal tissues, but only low levels of N-*myc* mRNA are detectable in most adult tissues. Thus, quantitative and qualitative differences in the levels of N-*myc* mRNA are demonstrable among different tissues and during development. N-*myc* mRNA is also detectable in several tumor cell types, including neuroblastoma, retinoblastoma, small-cell lung carcinoma, Wilms tumor, and primitive neuroepitheloma. Most tumor-derived established cell lines, including HeLa cells, have been previously shown not to accumulate N-*myc* mRNA in their cytoplasm (16, 22).

In this report, we describe studies that address the molecular basis of the differences in the specificity and level of expression of the N-*myc* gene among different cell types. Since previous studies failed to measure the relative rate of cellular N-*myc* gene expression in adult tissues from various established cell lines, it was possible that posttranscriptional control mechanisms could contribute to the expression of this mRNA. We have found, in fact, that the mouse N-*myc* gene is transcribed at equivalent levels in many adult mouse tissues examined and demonstrate that cell-specific differences in the level of N-*myc* RNA are the result of posttranscriptional control. Additional experiments using cultured tumor cell lines are presented which demonstrate that the DNA sequences necessary for this posttranscriptional control reside in the third exon and likely act to control the stability of N-*myc* RNA.

MATERIALS AND METHODS

Isolation of recombinant adenoviruses and preparation of virus stock. The viruses used included H5 *dl*309 (14), which has replicative characteristics in HeLa cells that are indistinguishable from those of wild-type adenovirus type 5; H5 *dl*313 (14), which has a deletion of the viral DNA sequences (second exon of E1A and the entire E1B gene coding sequences) extending from nucleotides 1338 to 3640; and a series of recombinant adenoviruses containing various regions of the mouse cellular N-*myc* gene cloned into the left end of the viral genome. The Ad-N-myc1 virus contains the leftmost 194 bp of adenovirus fused to N-*myc* sequences extending from nucleotides −1800 to +950, relative to the start site of N-*myc* transcription (11). The N-*myc* sequences at +950 were then ligated to the adenovirus sequences beginning at nucleotide 3328 (a *Bgl*II site) and extend to the right end of the viral genome. The Ad-N-myc3 virus contains the leftmost 1,338 bp of adenovirus (including the E1A gene cap site and 13S and 12S mRNA splice donor and acceptor sites) fused to a region of the mouse N-*myc* gene extending from nucleotides +4246 to +5726 [exon 3 and sequences 3′ to the poly(A) addition site]. The 3′ N-*myc* sequences were then fused to adenovirus sequences at nucleotide 3328, as for the Ad-N-myc1 virus. Both viruses were isolated by in vivo overlap recombination, using H3 *dl*309 parental viral genomes and human 293 cells to complement the viral E1A and E1B gene defects of the recombinant progeny viruses (14). The methodologies used to construct, isolate, characterize, and prepare high-titer virus stocks have been previously described (11).

Plasmid constructions and DNA transfection assays. Plasmid AdBgl3.8 was isolated by first cloning the adenovirus type 5 *Xho*I C fragment (nucleotides 0 to 5780) into the plasmid vector pMK2004. Viral sequences between 1338 (an

* Corresponding author.

*Xba*I site) and 3328 (a *Bgl*II site) were deleted to generate a plasmid containing a unique *Bgl*II site at this deletion junction. Initially, the mouse N-*myc* *Bam*Hi (−1800) and *Cla*I (+4246)-to-*Eco*RI (+5726) DNA fragments were cloned into plasmid AdBgl3.8 (see Fig. 5C). Subsequently, a series of DNA subclones from the N-*myc* *Cla*I-*Eco*RI fragment was cloned into this plasmid vector (9). These subclones included HC (+4246 to +4883), SH (+4883 to +5295), and RS (+5295 to +5726) (see Fig. 5C). For all constructs, the restriction enzyme-generated termini were converted to *Bam*HI sites by using DNA linkers. In most cases, both orientations were obtained. DNAs specific for the three mouse N-*myc* exons were prepared by subcloning *Eco*RI-*Bgl*II (−1800 to +950), *Bgl*II-*Bgl*II (+950 to +3464), and *Bgl*II-*Eco*RI (+3464 to +5726) DNAs into the Gemini plasmid vector. An additional plasmid was constructed in which an *Eco*RI-*Bam*HI restriction fragment extending from −1800 to +180 was subcloned into Gemini. This plasmid was linearized at the unique *Eco*RI site to generate antisense transcripts capable of scoring the mouse N-*myc* start site. Probes for the human N-*myc* gene were generated by subcloning an *Eco*RI-*Xho* and a *Xho*-*Bam*HI fragment from the human N-*myc* gene into Gemini. The *Xho*-*Bam*HI fragment contains a portion of the N-*myc* second exon; the *Eco*RI-*Xho*I plasmid is intronic (18).

Human neuroblastoma cell lines SKNMc (27) and G401 (1) and human HeLa cells were maintained as monolayer cultures and grown in Dulbecco modified Eagle medium supplemented with 10% fetal bovine serum. All three cell types were transfected at 50% confluence, using the calcium phosphate-DNA coprecipitation technique as previously described (6). The N-*myc*–adenovirus hybrid plasmids were cotransfected with a simian virus 40 enhancer–β-globin promoter-containing plasmid construct (SVglo), to control for variations in transfection efficiencies, into the three cell lines. After a glycerol shock (10% glycerol in phosphate-buffered saline) at 4 h posttransfection, cytoplasmic RNA was isolated at 36 h posttransfection. RNA was quantitated and mRNA levels were determined as previously described (11).

RNA preparation and analysis. RNAs from mouse tissues or mouse and human cell lines were prepared by the guanidinium thiocyanate technique of Chirgwin et al. (5). Cell pellets or tissues were dissolved in guanidium thiocyanate, and the RNA was pelleted through a cesium chloride cushion. For quantitation of specific RNA species, RNase T_2 protection assays were performed in which equivalent amounts of RNA were hybridized to specific uniformly labeled antisense RNA probes and subsequently trimmed with RNase T_2 (20). The resulting digestion products were resolved on a denaturing 5% polyacrylamide gel.

Transcription rates were measured by incubating nuclei isolated from mouse tissues or cell cultures with [^{32}P]UTP and cold GTP, CTP, and ATP to allow previously initiated RNA polymerase molecules to elongate (10). Nuclear RNA was isolated, followed by hybridization of equivalent numbers of counts to filters onto which cloned denatured DNAs had been spotted (10). After hybridization, the filters were treated with RNase T_1, RNase A, and proteinase K; washed; and exposed to autoradiography.

RESULTS

The mouse N-*myc* gene is transcribed in most mouse tissues. Eucaryotic gene expression can be regulated at multiple levels (8). While most tissue-specific genes are transcriptionally controlled, quantitative differences in the levels of individual mRNAs are often the result of posttranscriptional regulation (2, 10, 12, 23). To consider the level of gene expression relevant in the control of the mammalian N-*myc* gene, we first measured the transcription rate and steady-state mRNA levels of this gene in a variety of mouse tissues.

The levels of steady-state N-*myc* mRNAs were measured by use of an RNase T_2 protection assay specific for the first exon and transcriptional start site of the mouse N-*myc* gene. An *Eco*RI-*Bam*HI fragment was isolated from the mouse N-*myc* gene which spanned the predominant transcriptional start site (multiple start sites have been identified as a result of the absence of a well-defined TATA element [9]) and 180 bp of the first exon. This was cloned into the Gemini cloning vector. This plasmid was linearized with *Eco*RI, and an antisense transcript was synthesized by using SP6 RNA polymerase and hybridized to 20 μg of total RNA from fetal brain and from adult brain, liver, kidney, spleen, and placenta (Fig. 1A). A band of ~180 bp was protected in the fetal brain sample. N-*myc* RNA was not detectable in any other tissues. The levels of actin RNA were similar among these samples except fetal brain, which had an approximately threefold-higher level of actin RNA (23). These data are consistent with prior results documenting the size of the N-*myc* first exon, the relatively high level of expression in fetal brain, and the low levels of this mRNA in adult tissues (9).

In vitro nuclear run-on assays were performed, using nuclei isolated from these same tissues. An equivalent amount of [^{32}P]UTP-labeled nuclear RNA from each organ (fetal brain, adult brain, liver, spleen, kidney, and placenta) was hybridized to filters onto which were spotted DNAs specific for each of the three N-*myc* exons as well as actin (10). In each case, similar rates of N-*myc* transcription were observed among the tissues tested (Fig. 1B). This was determined by quantitating densitometric tracings and correcting signal intensity to that of the actin signal observed. Moreover, the signal intensity, when corrected for insert size, was equivalent for the exon 2 and 3 N-*myc* probes. With the exception of adult placenta, the exon 1 signal was greater than would have been predicted. Recent studies by Krystal et al. (19) most likely explain our findings. Their studies showed nearly equivalent rates of sense and antisense transcription across exon 1 of the human N-*myc* gene. Since our probes were double stranded, we were most likely scoring both of these signals with our exon 1 probe, which explains the greater than equimolar signal observed. The inserts from each of these clones hybridized to single bands on Northern (RNA) blots, suggesting that it was the single-copy N-*myc* sequences that were detected in this assay (data not shown). These findings demonstrate that the N-*myc* gene is transcribed in most, if not all, tissues at similar rates and that transcription is equimolar (when the exon 1 signal is corrected for the contribution of the antisense signal) across the transcription unit. Therefore, the lack of detectable N-*myc* mRNA in these mouse organs is likely the result of posttranscriptional regulation. In these experiments, two plasmid DNAs, pBR and Ad3.8, which is a pBR plasmid containing adenoviral sequences, were spotted to control for nonspecific hybridization signals.

The human N-*myc* gene is transcribed in many cultured cell types. To examine the regulatory level at which the N-*myc* gene is controlled in cultured cells, the transcription rates and steady-state levels of N-*myc* mRNA were measured in subconfluent monolayers of several human cell lines, including one neuroblastoma, IMR (29); a Wilms tumor, G401 (1);

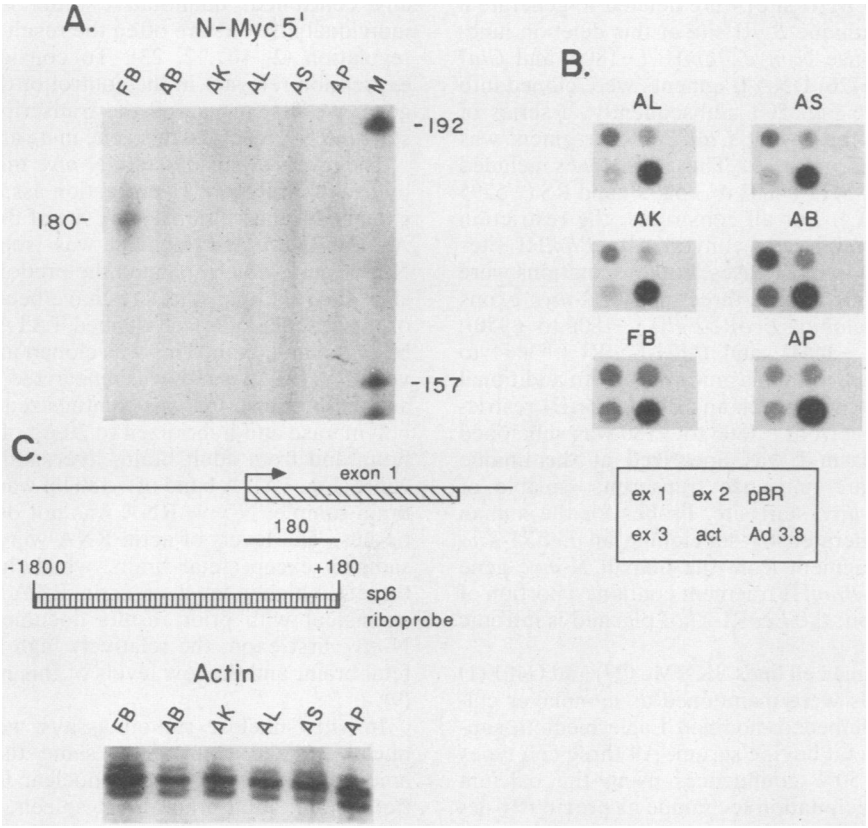

FIG. 1. Analysis of N-*myc* gene transcription and cytoplasmic mRNA accumulation in fetal and adult mouse tissues. Fetal mouse brains (FB) and adult mouse brains (AB), spleens (AS), livers (AL), kidneys (AK), and placentas (AP) were isolated, and total organ RNA was prepared (5). After purification through a cesium chloride cushion (see Materials and Methods), RNA from each tissue [20 μg of poly(A)-selected RNA] was hybridized to a uniformly ^{32}P-labeled SP6-generated antisense RNA probe (7.5×10^5 cpm) specific for the mouse N-*myc* 5′ end or the human γ-actin mRNA (20) (A). After hybridization and RNase T_2 digestion, the T_2-resistant hybrids were electrophoresed; autoradiographic exposure was for 48 h. The length of the protected RNA probe was determined by comparison with labeled DNA markers; these lengths are shown at the bottom of and on each side of panel A. To analyze the rates of N-*myc* gene expression among the various mouse organs (B), nuclei were isolated and labeled nuclear RNA was extracted after nascent-chain elongation in the presence of [^{32}P]UTP (10). Labeled RNA (10×10^6 cpm) was hybridized to dots of DNA (7 μg per dot) on nitrocellulose filters. Unpaired RNA was digested by RNase, and hybrids were detected by autoradiography. (C) Positions of the various DNAs. These DNAs include the mouse N-*myc* exon 1 (ex 1; −1800 to +950), exon 2 (ex 2; +950 to +3464), and exon 3 (ex 3; +3464 to +5726) (9), chicken β-actin, pBR322, and AdBgl3.8. The latter two DNAs were used as controls for nonspecific hybridization signals.

two primitive neuroepithelioma tumors; SKNMc (27) and SKNDw (27); and HeLa cells. The IMR neuroblastoma cell line has been shown to express high levels of N-*myc* mRNA as a result of amplification of the endogenous N-*myc* gene sequences; the Wilms tumor cells have been known to express high levels of N-*myc* RNA but have not amplified the N-*myc* gene; primitive neuroepithelioma tumors are reported to express low levels of the N-*myc* mRNA from a single copy of the N-*myc* gene; and HeLa cells do not synthesize steady-state N-*myc* RNA (22). Analysis of the levels of steady-state N-*myc* RNA are shown in Fig. 2A, in which a subclone of the human N-*myc* second exon was used as the template for the synthesis of [^{32}P]UTP-labeled antisense poly(A)-selected RNA and then hybridized at 59°C to RNA from each of these cell lines (24). An RNase T_2-protected RNA of 577 nucleotides was detected in all of the neuronal cell types. Consistent with prior reports, IMR expressed 100-fold higher levels of N-*myc* RNA than did G401 and SKNMc cells. In this experiment, SKNMc cells had higher levels of N-*myc* RNA than did G401 cells. The signal present in the HeLa cell lane of Fig. 2A is full-length probe which was improperly digested by RNase. HeLa cells failed to accumulate any N-*myc* mRNA, which is consistent with previous studies (22).

The rate of cellular N-*myc* gene transcription was measured in these cell lines by isolating nuclei from subconfluent monolayers and labeling previously initiated RNA chains with [^{32}P]UTP. Labeled RNA was isolated and hybridized to filters onto which had been spotted two subclones of the human N-*myc* gene that were derived from a 1-kb *Bam*HI-*Eco*RI fragment that includes a portion of intron 1 and exon 2. Subclones of this 1-kb fragment were ligated into Bluescript as a 600-bp *Bam-Xho* fragment that is intronic and a 500-bp *Xho-Eco*RI fragment that includes a small amount of intronic sequence and 400 bp of exon 2. Neither of these clones contains repetitive DNA, since both hybridize to single bands on Southern blots (data not shown). The *Xho-Eco*RI clone hybridized to a single RNA species on a Northern blot, and the *Bam-Xho* clone did not give a detectable signal when hybridized to RNA derived from these cell lines (data not shown).

Similar rates of transcription were seen among HeLa, SKNMc, and G401 cell lines even though HeLa cells do not accumulate cytoplasmic N-*myc* mRNA. The transcription

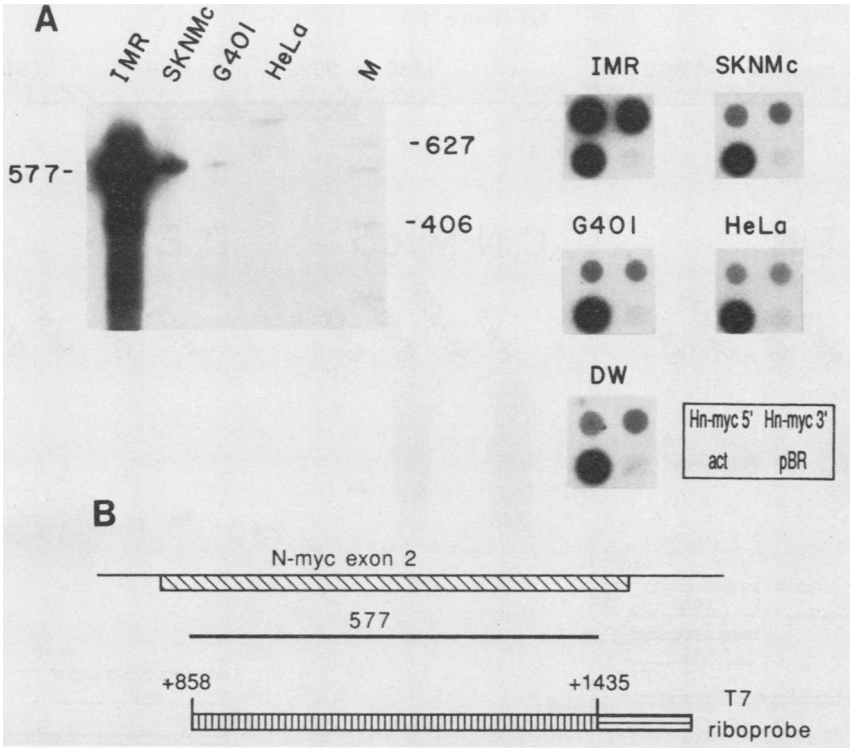

FIG. 2. (A) Analysis of N-*myc* gene transcription and cytoplasmic mRNA accumulation in established human cell lines. Cytoplasmic poly(A)-containing mRNA was isolated from the four human cell lines IMR (29), SKNMc (27), G401 (1), and HeLa. The steady-state accumulation of the cellular N-*myc* mRNAs in these cell lines was measured by using an RNase T_2 protection assay that detects the N-*myc* second exon. (B) Diagram of the SP6 probe and resulting RNase T_2 digestion product. This probe results in a protected RNA of 577 nucleotides. Transcription rates were determined as described in Materials and Methods by nuclear run-on assay. The DNAs spotted on the nitrocellulose filters include Hn-myc5′ (17), Hn-myc3′ (17), chicken β-actin, and pBR322.

rate in the cells with amplified N-*myc* sequences (IMR), however, was 10-fold higher than that in cell lines with a single copy of the N-*myc* gene. This increased transcription rate of the N-*myc* gene in IMR cells did not completely account for the 100-fold difference in the level of steady-state mRNA in these cells. Thus, posttranscriptional control may account for qualitative and quantitative differences in the levels of N-*myc* RNA among cell lines with a single copy of the endogenous N-*myc* gene.

The mouse N-*myc* promoter functions in cultured human cell lines regardless of the endogenous levels of N-*myc* mRNAs. These results predict that an exogenous N-*myc* promoter should function at equivalent rates in all cells regardless of whether endogenous steady state N-*myc* RNA is present. To monitor the activity of the mouse-N-*myc* promoter in cultured cells, we made use of a recombinant adenovirus expression vector. This vector was previously used to demonstrate cell-specific expression of the rat albumin and mouse immunoglobulin promoters (11). A 2.75-kbp *Eco*RI-*Bgl*II fragment of the mouse N-*myc* gene which extends from nucleotides −1800 to +950 was subcloned into the *Bgl*II site of the parent plasmid, AdBgl6, using *Bgl*II linkers. AdBgl6 is a modified plasmid that includes adenoviral sequences from 0 to 15.5 map units (11). In this plasmid, adenoviral DNA sequences between bp 194 and 3320 have been deleted and replaced with the *Bgl*II linker. In the resulting plasmid, the E1A gene as well as the E1B promoter and first exon have been removed and replaced by the N-*myc* promoter and first exon. In this construct, the N-*myc* promoter directs the synthesis of a fusion mRNA in which the mouse N-*myc* first exon is spliced to the adenoviral E1B second exon. These sequences were then introduced into a full-length adenovirus genome by in vivo overlap recombination, and the resulting recombinant virus was named Ad-N-myc1 (Fig. 3A). Both of the alternative leader sequences of the N-*myc* first exon were included in this construct (28).

In our initial experiments, subconfluent monolayers of each of the cultured cell lines shown in Fig. 2 were infected at 20 PFU per cell with Ad-N-myc1 (Fig. 3A). Cytoplasmic RNA was prepared from infected cells at 8 h postinfection. RNase protection assays were performed by hybridizing antisense ^{32}P-labeled RNA probes corresponding to the viral E1B gene (Fig. 3B), N-*myc* 5′ end (Fig. 3C), viral E2A gene (Fig. 3D), and human β-actin gene (data not shown) to RNA (20 μg) from infected G401, SKNMc, SKNDw, and HeLa cells (11). Steady-state levels of N-*myc*-transcribed E1B RNA were present in the G401, SKNMc, and HeLa cell lines; in fact, higher levels of E1B were demonstrable in HeLa cells (which do not accumulate endogenous N-*myc* mRNA) (Fig. 3B). To control for variations in virus uptake by these cell lines, the level of another viral gene, E2A, was measured by using an E2A riboprobe. We could score an E2A mRNA signal in all of the cell lines (Fig. 3D), suggesting that all of the cell types could be infected. An analysis of cellular actin mRNA levels from the different cell lines revealed similar levels, suggesting that the integrity and quantitation of the RNAs were correct (data not shown). To demonstrate that the correct N-*myc* initiation sites were used on the viral templates, the infected-cell RNA was hybridized to the probe depicted in Fig. 1 and corresponding

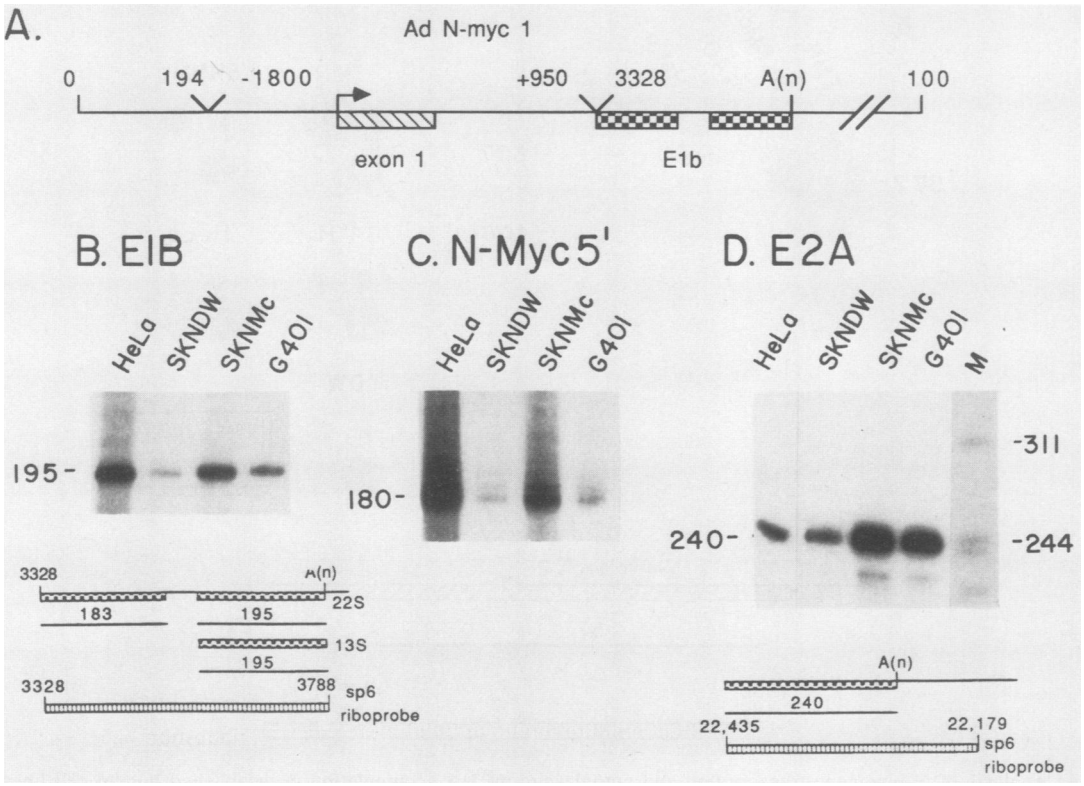

FIG. 3. Demonstration that expression of the mouse N-*myc* gene from an adenoviral vector results in N-*myc* exon 1–E1B hybrid mRNA accumulation in HeLa cells. The construction, isolation, and genotypic characterization of the Ad-N-myc1 virus are described in Materials and Methods. Mouse N-*myc* gene sequences extending from nucleotides −1800 to +950 (including the N-*myc* transcriptional start site and first exon) were inserted into the left end of the adenovirus genome, resulting in a deletion of the viral E1A gene and 5′ portion of the E1B gene (A). Symbols: ▨, N-*myc* exonic sequences; ▩, adenovirus E1B exons. Cytoplasmic RNA was isolated from HeLa, SKNDw, SKNMc, and G401 cells infected with Ad-N-myc1 virus (20 PFU per cell) at 8 h postinfection, and 20 μg was hybridized to ^{32}P-labeled antisense RNA probes (7.5×10^5 cpm) representing the viral E1B (B) and E2A (D) genes and mouse N-*myc* 5′ cap site and exon 1 (C). After RNase T_2 digestion, the T_2-resistant hybrids were analyzed on 5% denaturing acrylamide gels. The lengths (in nucleotides) of the protected RNA probes for each transcription unit are indicated in the line drawings below the panels. The SP6 riboprobe used to detect N-*myc* mRNA is described in the legend to Fig. 1. Cell lines are indicated above the lanes; lane M contained labeled DNA markers (sizes are indicated in nucleotides).

to the first exon of the mouse N-*myc* gene. A 180-nucleotide RNA (although multiple RNA species are observed as a result of multiple start sites) characteristic of the correctly initiated mouse N-*myc* gene was scored in all of the virus-infected cell lines, and the amount of this protected RNA was proportional to the levels of E1B mRNA observed in each cell type. This result was expected, since both assays scored the same mRNAs. This probe was shown not to cross-react with the endogenous human N-*myc* RNAs expressed in the SK and G401 cell lines (data not shown). We can also conclude that viral DNA replication had not occurred in any of the virus-infected cell lines, since the activity of the viral pIX promoter located in the E1B gene sequences could not be detected (11).

The results depicted in Fig. 3 demonstrate that a correctly initiated N-*myc* fusion RNA is synthesized in these four cell lines. Thus, both exogenous and endogenous N-*myc* promoters appear to function at equivalent rates among three cell lines that differ in the accumulation of steady-state levels of the endogenous human N-*myc* mRNA.

Sequences 5′ to the N-*myc* poly(A) addition site confer cell-specific expression. After examining the sequence of the N-*myc* gene, we noted an A+T-rich sequence in the third exon that resembled the sequence seen in other genes that are controlled at the level of RNA stability. Furthermore, the Ad-N-myc1 virus studies suggested that the N-*myc* sequences in the first exon were not responsible for the cell-specific stability of the N-*myc* mRNAs. We next tested the possibility that defined sequences were important in N-*myc* gene control by again using an adenovirus vector. First, a plasmid was constructed in which the viral E1A gene second exon and poly(A) site were deleted at an *Xba*I site at bp 1338 and were replaced by a *Cla*I-*Eco*RI fragment (nucleotides +4246 to +5726) of the mouse N-*myc* gene which contained the N-*myc* third exon and poly(A) site (Fig. 4) (11). This plasmid, in which the E1A promoter directs the synthesis of the N-*myc* 3′ end, was incorporated into an intact adenovirus by homologous recombination. The genomic organization of the Ad-N-myc3 virus is shown in Fig. 4. Two additional viruses were used in these experiments as a control: H5 *dl*309, which contains the wild-type E1A gene, and H5 *dl*313, in which the E1A second exon and poly(A) site were deleted and replaced by the E1B second exon and poly(A) site (Fig. 4A) (14). These viruses were then used to infect G401, HeLa, IMR, and SKNMc cells at a multiplicity of 20 PFU per cell. Whole-cell RNA was prepared 8 h postinfection and hybridized to a ^{32}P-labeled antisense E1A probe as well as to an actin probe.

The effect of the N-*myc* third exon on RNA stability was monitored by comparing the level of E1A mRNA synthe-

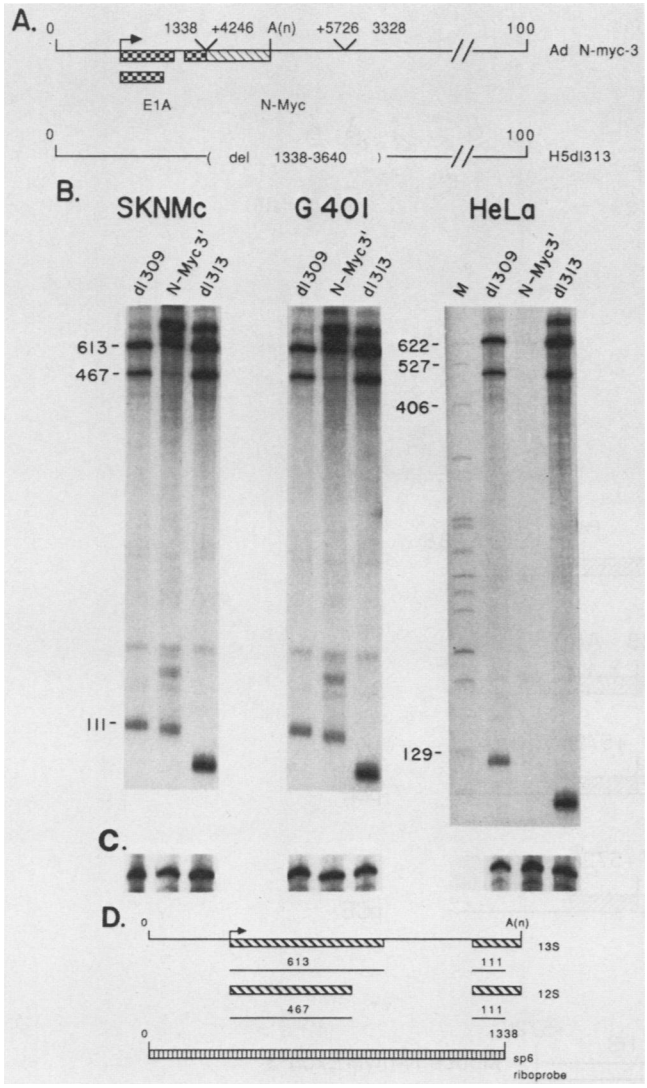

FIG. 4. Demonstration that sequences in the 3′ untranslated region of the mouse N-*myc* gene confer message stability in the appropriate cell type. The construction, isolation, and genotypic characterization of the Ad N-*myc3* virus (A) are described in Materials and Methods. Mouse N-*myc* gene sequences extending from nucleotides +4246 to +5726 [including the third exon and poly(A) addition sequence] were inserted 3′ to the E1A cap site in the second exon of the E1A gene. Symbols: ▩, adenovirus E1A exonic sequence; ▨, mouse N-*myc* sequence. H5 *dl*313 virus has been previously described (14) and contains a deletion (represented by parentheses) of the 3′ region of the E1A gene and the E1B gene cap site. (B) mRNA analysis. Cytoplasmic RNA was isolated from virus-infected (as indicated above the lanes) SKNMc, G401, and HeLa cells (20 PFU per cell for 8 h) and analyzed for viral E1A mRNA accumulation, using an SP6 riboprobe that hybridizes to the E1A 13S and 12S mRNAs (see panel D for lengths of the protected RNAs). (C) Determination of actin mRNA levels in all infected cells to control for variations in RNA preparation or quantitation.

sized from the Ad-N-myc3 virus (containing the N-*myc* 3′ end) with the level synthesized from the control virus templates (which make use of either the wild-type E1A or E1B 3′ end). In HeLa cells, the level of E1A mRNA synthesized from the Ad-N-myc3 virus E1A gene was undetectable, while abundant transcripts were synthesized from the control template (Fig. 4B; scored as unspliced and 13S spliced RNA species). In SKNMc and G401 cells, the N-*myc* third exon reduced the level of E1A RNA two- to threefold relative to the control level. For all studies, the levels of actin mRNA were quantitated to control for variations in RNA. These results demonstrate that RNA sequences in the N-*myc* third exon can posttranscriptionally regulate the levels of these hybrid mRNA species in a cell-specific fashion and that these sequences are also functional in a recombinant adenovirus. The activity of this element appears to account for at least part of the qualitative and quantitative differences in the expression of N-*myc* RNA. Nevertheless, these experiments do not distinguish whether the differences in the levels of E1A RNA synthesized from the Ad-N-myc3 virus are the result of differential RNA stability or effects on the efficiency of polyadenylation or nuclear cytoplasmic mRNA transport.

A 600-bp sequence in the N-*myc* third exon is likely responsible for N-*myc* RNA stability. The results from the Ad-N-myc3 virus studies suggested that N-*myc* gene expression is controlled to a large extent by sequences in the third exon. To further delineate the DNA sequences involved in the regulation of this gene, a series of constructs was made in which a number of subgenomic fragments of the N-*myc* third exon were introduced into the second exon of the E1A gene in a plasmid containing the wild-type E1A promoter and E1B poly(A) addition sites (Fig. 5C). In initial experiments, restriction fragments of the N-*myc* gene were ligated into the adenovirus gene sequences between nucleotides 1338 (in the E1A gene second exon) and 3328 in plasmid pE1A, using *Xba*I linkers (11). Plasmid pBE fused the E1A second exon to a *Bam*HI site in the N-*myc* first exon (+185) and included all three N-*myc* exons and the poly(A) addition site (+5726). In plasmid pCE, the E1A second exon was ligated to a *Cla*I site in the N-*myc* third exon (+4246) and included only the third exon and poly(A) addition site (+5726). pBE therefore contains nearly the entire N-*myc* coding sequence, and pCE contains only the N-*myc* third exon. Both plasmids as well as two control plasmids, wild-type E1A plasmid (Ad) and a plasmid in which E1A mRNA utilizes the E1B poly(A) site (AdΔ), were introduced separately into HeLa and SKNMc cells by $CaPO_4$ transfection. After 36 h, cytoplasmic RNA was prepared and assayed for the level of E1A RNAs, using an RNase T_2 protection assay. A control plasmid, SVglo, which contains the simian virus 40 enhancer upstream of the mouse β-globin promoter and directs the synthesis of E1B RNA, was cotransfected in each case as an internal control for transfection efficiency (6).

The level of E1A RNA synthesized from pBE and pCE was compared with that synthesized from the control plasmids. In this experiment, the levels of the E1A–N-*myc* hybrid RNA synthesized from pBE and pCE were considerably lower in HeLa cells than in SKNMc cells after correction for transfection efficiency by using the SVglo control plasmid (Fig. 5A). These data confirm the results for the recombinant adenovirus and also suggest that sequences between the *Bam* site (+185) in the first exon of the N-*myc* gene and the *Cla* site (+4246) in the third exon do not further diminish the level of RNA synthesized in HeLa cells.

To further elucidate which exon 3 sequences were responsible for the diminished level of mouse N-*myc* expression in HeLa cells, restriction fragments from the N-*myc* third exon were subcloned into the pE1A plasmid in the sense and antisense orientations. These plasmids were cotransfected into HeLa cells along with the SVglo plasmid control. The level of E1A expression was scored for each of these plasmids and compared with the wild-type E1A level. In this

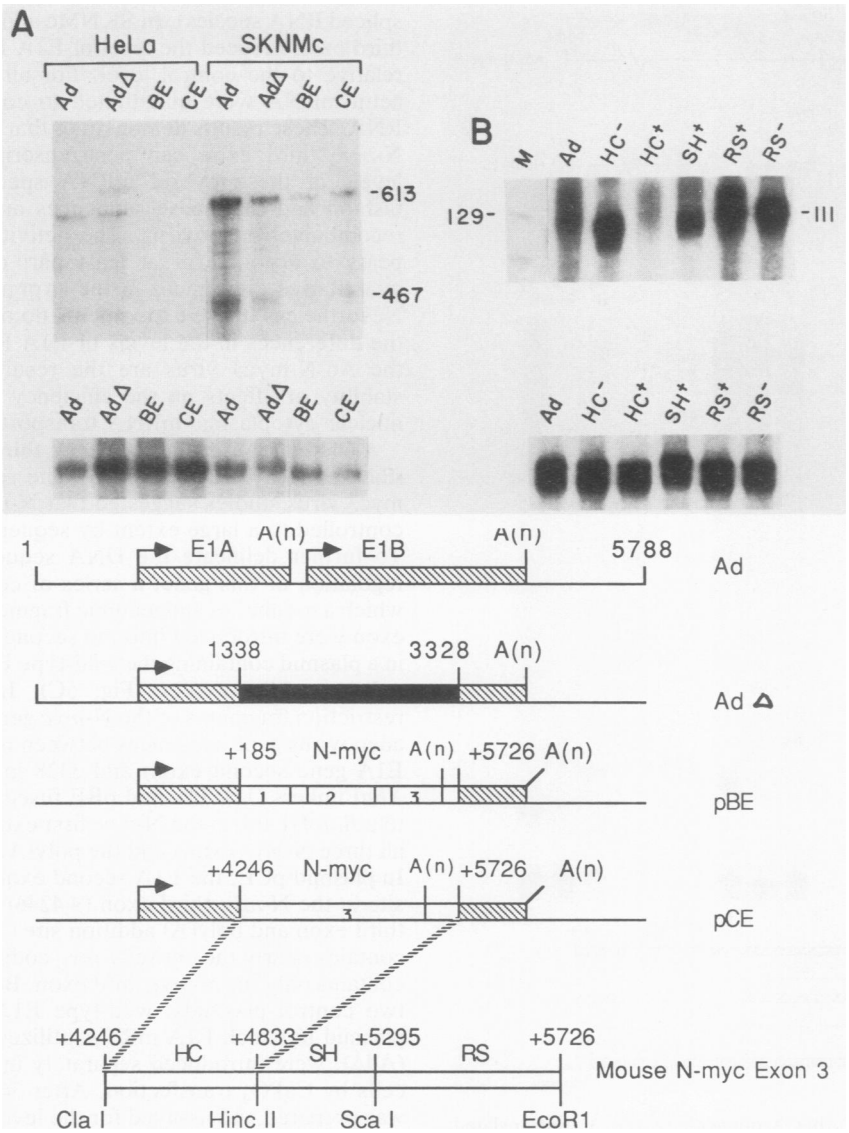

FIG. 5. Demonstration that a sequence in the 3′ untranslated region of the mouse N-*myc* mRNA confers cytoplasmic instability in human HeLa cells. The plasmid constructs used in the DNA transfection assays are depicted in panel C. Plasmid Ad contains adenovirus type 5 sequences extending from bp 0 to 5788 and contains the viral E1A and E1B gene regions (▨). Plasmid AdΔ contains these same viral sequences with a deletion (■) extending from bp 1338 to 3328. As a result, only the E1A cap site, E1A exon 1 and part of exon 2, and exon 2 and the poly(A) addition site for the E1B gene are retained on this plasmid. Plasmids pBE and pCE were derived from plasmid AdΔ and contain different regions of the mouse N-*myc* coding regions (numbered boxes representing the N-*myc* exons). The mouse N-*myc* exon 3 region is shown below, along with the restriction endonuclease-generated DNA fragments that were cloned in either orientation into the AdΔ plasmid vector. The hatched lines illustrate how the HC plasmid was constructed, for example. These plasmids were all named according to the restriction enzymes used for their isolation. The various constructs were transfected into SKNMc and HeLa cells along with the control plasmid SVglo, and cytoplasmic RNA was isolated and assayed after 36 h with antisense RNA probes representing the E1A 5′ end (A), the E1A 3′ end (B), and mouse β-globin exon 1 (shown below panels A and B) (6). Sizes (in nucleotides) of the RNase T_2 digestion products are indicated.

experiment (Fig. 5B), the levels of E1A mRNA synthesized from the wild-type plasmid 36 h posttransfection were equivalent among the wild-type E1A control and all plasmids except pHC+ (nucleotides +4246 to +4883). Steady-state RNA produced from this plasmid was reduced by a factor of 10 in HeLa cells. However, the plasmid that contained a copy of this sequence in the sense orientation functioned at a rate equivalent to the wild-type E1A rate in G401 and SKNMc cells (data not shown). The restriction fragment that conferred this effect did not include the poly(A) addition site. These data demonstrated that the posttranscriptional control of the N-*myc* gene is conferred by the activity of DNA sequences in the 3′ untranslated region of this gene.

DISCUSSION

In this study, we investigated the mechanism by which the level of N-*myc* RNA is regulated among different cell types in vivo and in cultured cells. Our results suggest that the cell-specific regulation of the N-*myc* gene is effected primarily at the posttranscriptional level. The supporting evidence for this conclusion includes the following: (i) the equivalent

rates of transcription of the N-*myc* gene, obtained by using in vitro nuclei, among all cell types tested irrespective of the levels of steady-state endogenous RNA (also, there is no evidence to suggest that premature termination is relevant in the control of the N-*myc* gene, as has been reported for c-*myc* [3], since transcription is equimolar across the transcription unit in brain, placenta, liver, kidney, and spleen); (ii) the equivalence of the activity of the N-*myc* promoter in directing the synthesis of a reporter gene even in HeLa cells, which do not accumulate cytoplasmic N-*myc* mRNA; and (iii) the demonstration that specific sequences in the N-*myc* third exon can confer cell-specific N-*myc* mRNA stability when inserted into viral and plasmid constructs which are transcribed at equivalent rates among HeLa, SKNMc, and G401 cells.

These results are similar in some respects to those of Zimmerman et al. (31), who demonstrated that appropriate expression of the transfected mouse N-*myc* gene is not observed in cultured cells, since cells which failed to express human N-*myc* RNA still expressed the mouse N-*myc* RNA. However, these studies showed that sequences from the third exon of the N-*myc* gene did not alter the level of expression of the reporter gene (31), as we have reported. Of further interest is the observation that N-*myc* sequences that lack the third exon (which we have shown to destabilize the mRNA in cultured cells) still act to direct cell-specific expression of N-*myc* in transgenic animals (32). However, it is not entirely clear from these studies whether the expression of the transgene is the result of transcriptional or posttranscriptional control. The reason for this discrepancy is not entirely clear, although the choice of promoter and efficiency of mRNA translation may influence the effect of N-*myc* exon 3 sequences on mRNA levels. Wilson and Treisman (30) have suggested that the half-life of the cellular *fos* mRNA is determined by the translation efficiency of the mRNA itself. In our studies, the E1A–N-*myc* fusion mRNAs may be more efficiently translated than the endogenous N-*myc* mRNAs and consequently may turn over rapidly as a result of the exon 3 sequences.

In additional experiments, we have localized the sequences responsible for the regulated expression of N-*myc* RNA to a 600-bp fragment of the N-*myc* third exon. Cell-specific expression of the gene does not appear to require any additional sequences outside the third exon, since a construct which includes all three exons and extends from a *Bam*HI site in the first exon to the *Eco*RI site downstream of the third exon is expressed at a rate equivalent to that of constructs which include only sequences from the third exon. Thus, it appears that sequences from the N-*myc* third exon are both necessary and sufficient for the regulated and cell-specific expression of this RNA.

Previous reports have demonstrated, however, that the regulated expression of some RNAs, particularly those with a short half-life, can be the result of differences in RNA stability (2, 4, 7, 15, 26). These reports have noted that mRNAs which are regulated by differences in RNA stability often have A+U-rich sequences in the 3′ untranslated region of the RNA. mRNAs in this class have included certain lymphokines, cytokines, and proto-oncogenes and often have a characteristic TTATTTATT consensus sequence in the 3′ untranslated region (4). The mouse N-*myc* gene appears to be yet another member of this group. The DNA sequences of the N-*myc* third exon do indeed contain several A+T-rich regions, although the TTATTTATT consensus sequence was not noted in the sequences which are responsible for differences in the stability of the N-*myc* RNA. c-*myc* RNA is also regulated by differences in RNA stability, and this mRNA also does not contain a TTATTTATT sequence. The c-*myc* 3′ untranslated region does include an uninterrupted stretch of 11 U residues (15). Similarly, the N-*myc* RNA has an uninterrupted stretch of 14 U residues (15). It is not clear whether this sequence represents a new motif that regulates RNA stability. A more refined deletion analysis of the sequences in this region that includes the testing of linker-scanning mutants should help localize further the RNA sequences that are required for this effect and determine whether a poly(U) tract can function to destabilize specific RNAs.

In conclusion, we have demonstrated that cell-specific expression of N-*myc* RNA is likely the result of posttranscriptional control. The sequences that confer this regulation are present in the third exon and include a poly(U) tract, in common with sequences of the c-*myc* gene that control RNA stability. Finally, we have demonstrated that posttranscriptional gene control can be demonstrated in an adenovirus vector. The use of pulse-chase and approach-to-steady-state methods in cells infected with these viruses may make it possible to study the kinetics of this process.

ACKNOWLEDGMENTS

We thank Fred Alt for providing the mouse N-*myc* gene. We also thank L. Cousseau for her expert help in preparing the manuscript.

This work was aided by a grant from the American Cancer Society (JFRA-235 to L.E.B.), by Public Health Service grant CA49707-10 (to L.E.B.) from the National Institutes of Health, and by a grant from the Howard Hughes Medical Institute (to J.F.).

LITERATURE CITED

1. **American Type Culture Collection.** 1988. ATCC catalogue of cell lines and hybridomas, 6th ed. American Type Culture Collection, Rockville, Md.
2. **Babich, A., and J. R. Nevins.** 1981. The stability of early adenovirus mRNA is controlled by the viral 72 kd DNA-binding protein. Cell **26**:371–379.
3. **Bentley, D. L., and M. Groudine.** 1988. Sequence requirements for premature termination of transcription in the human c-myc gene. Cell **53**:245–256.
4. **Caput, D., B. Beutler, K. Hartog, R. Thayer, S. Brown-Shimer, and A. Cerami.** 1986. Identification of a common nucleotide sequence in the 3′-untranslated region of mRNA molecules specifying inflammatory mediators. Proc. Natl. Acad. Sci. USA **83**:1670–1674.
5. **Chirgwin, J. M., A. E. Pryzbyla, R. MacDonald, and W. J. Rutter.** 1979. Isolation of biologically active ribonucleic acid from sources enriched in ribonuclease. Biochemistry **18**:5294–5299.
6. **Costa, R. H., E. Lai, D. R. Grayson, and J. E. Darnell.** 1988. The cell-specific enhancer of the mouse transthyretin (prealbumin) gene binds a common factor at one site and a liver-specific factor(s) at two other sites. Mol. Cell. Biol. **8**:811–90.
7. **Dani, C. H., J. M. Blanchard, M. Piechaczyk, S. El Sabouty, L. Marty, and P. H. Jeanteur.** 1984. Extreme instability of myc mRNA in normal and transformed human cells. Proc. Natl. Acad. Sci. USA **81**:7046–7050.
8. **Darnell, J. E., Jr.** 1982. Variety in the level of gene control in eukaryotic cells. Nature (London) **297**:365–371.
9. **DePinho, R. A., E. LeGouy, L. B. Feldman, N. E. Kohl, G. D. Yancopoulos, and F. W. Alt.** 1986. Structure and expression of the murine N-myc gene. Proc. Natl. Acad. Sci. USA **83**:1827–1831.
10. **Derman, E., K. Krauter, L. Walling, C. Weinberger, M. Ray, and J. E. Darnell, Jr.** 1981. Transcriptional control in the production of liver-specific mRNAs. Cell **23**:731–739.
11. **Friedman, J. M., L. E. Babiss, D. F. Clayton, and J. E. Darnell.** 1986. Cellular promoters incorporated into the adenovirus genome: cell specificity of albumin and immunoglobulin expres-

sion. Mol. Cell. Biol. 6:3791–3797.
12. **Friedman, J. M., E. Cheng, and J. E. Darnell.** 1984. Gene expression in regenerating liver. J. Mol. Biol. **179**:37–53.
13. **Jakobovits, A., M. Schwab, J. M. Bishop, and G. R. Martin.** 1985. Expression of N-myc in teratocarcinoma stem cells and mouse embryo. Nature (London) **318**:188–191.
14. **Jones, N., and T. Shenk.** 1979. Isolation of adenovirus type 5 host range deletion mutants defective for transformation in rat embryo cells. Cell **17**:683–689.
15. **Jones, T. R., and M. D. Cole.** 1987. Rapid cytoplasmic turnover of c-*myc* mRNA: requirement of the 3′ untranslated sequences. Mol. Cell. Biol. **7**:4513–4521.
16. **Kohl, N., C. Gee, and F. Alt.** 1984. Activated expression of the N-myc gene in human neuroblastomas and related tumors. Science **226**:1335–1337.
17. **Kohl, N., N. Kanda, R. Schreck, G. Bruns, S. Latt, F. Gilbert, and F. Alt.** 1983. Transposition and amplification of oncogene-related sequences in human neuroblastomas. Cell **35**:359–367.
18. **Kohl, N. E., E. Legouy, R. A. DePinho, P. D. Nisen, R. K. Smith, C. E. Gee, and F. W. Alt.** 1986. Human N-myc is closely related in organization and nucleotide sequence to c-myc. Nature (London) **319**:73–77.
19. **Krystal, G. W., B. C. Armstrong, and J. F. Battey.** 1990. N-*myc* mRNA forms an RNA-RNA duplex with endogenous antisense transcripts. Mol. Cell. Biol. **10**:4180–4191.
20. **Melton, D., P. S. Krieg, M. R. Rebagliati, T. Maniatis, K. Zinn, and M. R. Green.** 1984. Efficient in vitro synthesis of biologically active RNA and RNA hybridization probes from plasmids containing a bacteriophage SP6 promoter. Nucleic Acids Res. **12**:7035–7056.
21. **Nau, M. M., B. J. Brooks, J. Bettey, E. Sausville, A. F. Bazdar, I. R. Kirsch, O. W. McBride, V. Bertness, G. F. Hollis, and J. D. Minna.** 1985. L-myc, a new myc-related gene amplified and expressed in human small cell lung cancer. Nature (London) **318**:69–73.
22. **Nisen, P. D.** 1986. N-myc expression in Wilms' tumors. Cancer Res. **46**:6217–6222.
23. **Powell, D. J., J. M. Friedman, A. J. Oulette, K. S. Krauter, and J. E. Darnell, Jr.** 1984. Transcriptional and post-transcriptional control of specific messenger RNAs in adult and embryonic liver. J. Mol. Biol. **179**:21–35.
24. **Schwab, M., K. Alitalo, K.-H. Klempnauer, H. E. Varmus, J. M. Bishop, F. Gilbert, G. Brodeur, M. Goldstein, and J. Trent.** 1983. Amplified DNA with limited homology to myc cellular oncogene is shared by human neuroblastoma cell lines and a neuroblastoma tumour. Nature (London) **305**:245–248.
25. **Schwab, M., H. E. Varmus, and J. M. Bishop.** 1985. Human N-myc gene contributes to neoplastic transformation of mammalian cells in culture. Nature (London) **316**:160–162.
26. **Shaw, G., and R. Kamen.** 1986. A conserved AU sequence from the 3′ untranslated region of GM-CSF mRNA mediates selective mRNA degradation. Cell **46**:659–667.
27. **Spengler, B. A., J. L. Bieder, L. Helson, and L. S. Freedman.** 1973. Morphology and growth, tumorigenicity and cytogenetics of human neuroblastoma cells established in vitro. In Vitro **8**:410.
28. **Stanton, L. W., and J. M. Bishop.** 1987. Alternative processing of RNA transcribed from *NMYC*. Mol. Cell. Biol. **7**:4266–4272.
29. **Tumilowicz, J. J., W. W. Nichols, J. J. Cholon, and A. E. Greene.** 1970. Definition of a continuous cell line derived from neuroblastoma. Cancer Res. **30**:2110–2118.
30. **Wilson, T., and R. Treisman.** 1988. Removal of poly(A) and consequent degradation of c-fos mRNA facilitated by 3′ AU-rich sequences. Nature (London) **336**:396–399.
31. **Zimmerman, K., E. Legouy, V. Stewart, R. DePinho, and F. W. Alt.** 1990. Differential regulation of the N-*myc* gene in transfected cells and transgenic mice. Mol. Cell. Biol. **10**:2096–2103.
32. **Zimmerman, K. A., G. D. Yancopoulos, R. G. Collum, R. K. Smith, N. E. Kohl, K. A. Denis, M. M. Nau, O. N. Witte, D. Toran-Allerand, C. E. Gee, J. D. Minna, and F. W. Alt.** 1986. Differential expression of myc family genes during murine development. Nature (London) **319**:780–783.